Science and Technology Indonesia
e-ISSN:2580-4391 *p*-ISSN:2580-4405
Vol. 8, No. 3, July 2023

Research Paper

Increasing the Solubility and Anti-Inflammatory Activity of Curcumin by Cocrystallization

Yudi Wicaksono[1]*, Kuni Zu'aimah Barikah[1], Amanda Della Yudatama[1], Havidhatul Maulia[1], Nuri[2], Dwi Setyawan[3]

[1]*API and Excipient Research Group, Faculty of Pharmacy, University of Jember, Jember, 68121, Indonesia*
[2]*Bio-Active Natural Product Development Research Group, Faculty of Pharmacy, University of Jember, Jember, 68121, Indonesia*
[3]*Faculty of Pharmacy, Airlangga University, Surabaya, 60286, Indonesia*
***Corresponding author**: yudi.farmasi@unej.ac.id

Abstract
Curcumin (CUR) is a polyphenolic compound that exhibits potent anti-inflammatory activity. However, only a tiny amount of CUR is absorbed during oral administration, which is because CUR is difficult to dissolve in water. The aim of the research was to increase the solubility of CUR through the cocrystallization technique using isonicotinamide coformer (INIC) by solvent evaporation. Cocrystal characterization was carried out using a powder X-ray diffractometer (PXRD), a differential scanning calorimeter (DSC), a Fourier transform infrared spectrometer (FTIR), and a scanning electron microscope (SEM). Solubility was evaluated using the shaking method, while the anti-inflammatory activity test was carried out using the carrageenan-induced mouse leg edema method. The resulting CUR-INIC (1:1) cocrystal has a diffractogram with new diffraction peaks of 2θ at 15.00, 16.22, and 22.89° compared to the individual diffractograms of CUR and INIC. In the cocrystal, CUR and INIC form intermolecular interactions of hydrogen bonds, resulting in a new solid phase with a melting point of 160.1°C. The solubility of the CUR-INIC cocrystal in water was 73.1±0.23 μg/mL, which increased 14 times compared to the solubility of initial CUR, which was only 5.05±0.07 μg/mL. The CUR-INIC cocrystal showed a percentage of edema inhibition in mice (5 hours) 130% more potent than that of initial CUR. Therefore, CUR-INIC cocrystals can be used to improve CUR solubility to obtain more excellent anti-inflammatory effects.

Keywords
Curcumin, Solubility, Anti-Inflammatory, Cocrystals, Isonicotinamide

Received: 23 January 2023, Accepted: 1 July 2023
https://doi.org/10.26554/sti.2023.8.3.501-508

1. INTRODUCTION

Curcumin (CUR) is a polyphenol compound with various biological activities such as anti-inflammatory, antioxidant, and anti-tumor (Sohn et al., 2021). CUR has been shown to have potent anti-inflammatory effects in various inflammatory diseases in clinical trials. The anti-inflammatory effect of CUR is considered to be the basis of various pharmacological activities which play an essential role in the treatment of various diseases. Therefore, CUR is considered one of the natural compounds with tremendous potential in treating diseases (Peng et al., 2021). However, until now, the use of CUR as a therapeutic drug is still constrained by pharmacokinetics (Sohn et al., 2021; Tabanelli et al., 2021; Hakim et al., 2021). CUR given orally is very little absorbed in the gastrointestinal tract, so its bioavailability to achieve pharmacological effects is less than 1% (Suresh and Nangia, 2018; Peng et al., 2021). One reason for the low absorption of CUR in the gastrointestinal tract is that CUR is very slightly soluble in water (<8 mg/L) (Suresh and Nangia, 2018; Zhang et al., 2023). The structure of the CUR molecule has two aromatic ring systems with o-methoxy phenolic groups, connected by seven carbon linkers consisting of an α,β-unsaturated β-diketone groups so that it is hydrophobic and difficult to dissolve in water (Priyadarsini, 2014; Suresh and Nangia, 2018).

Various techniques have been used to increase the solubility of active pharmaceutical ingredients (API), one of which is the formation of multicomponent solids (Sohn et al., 2021; Sanphui and Bolla, 2018; Fang et al., 2021). A multicomponent solid is formed from an API and a coformer, resulting in a new solid phase (Haneef and Chadha, 2017; Palanisamy et al., 2019). The API can be prepared into a multicomponent solid with certain coformer so the solubility can increase (Haneef and Chadha, 2017; Chavan and Shastri, 2018; Wicaksono et al., 2021; Anggraini et al., 2022).

Cocrystallization is an exciting and attractive technique for forming multicomponent solids to increase the solubility of API (Karimi-Jafari et al., 2018). Cocrystals are multicomponent

solids formed by two or more types of molecules with non-covalent interactions such as hydrogen bonds, van der Waals interactions, and ϕ-ϕ interactions (Haneef and Chadha, 2017; Sanphui and Bolla, 2018; Wicaksono et al., 2020). Cocrystals can increase the solubility of crystalline API through the mechanism of decreasing crystal lattice energy so that API in crystalline solids is more easily hydrated by water molecules (Ozaki et al., 2014; Docherty et al., 2015; Bergström and Larsson, 2018). The increased solubility of API by cocrystallization has thermodynamic advantages because its formation is usually spontaneous, the resulting solid is energetically more stable than its pure form, and the cocrystal structure is separate from the constituent components (Maheshwari et al., 2009; Fischer et al., 2016; Taylor and Day, 2018). Another critical advantage of cocrystallization is that the API and coformer interact through non-covalent interactions so that they do not change the molecular structure and pharmacological activity of the API (Haneef et al., 2021; Guo et al., 2021; Acebedo-Martínez et al., 2022).

The aim of this research is to increase the solubility of CUR by cocrystallization technique so that CUR becomes more easily absorbed in the gastrointestinal tract and has greater bioavailability to achieve therapeutic effects as an anti-inflammatory (Suresh and Nangia, 2018; Gao et al., 2019; Chen et al., 2020; Peng et al., 2021). The CUR molecule has a beta-diketol group and two phenolic groups, which are known to be highly reactive in forming intermolecular interactions of hydrogen bonds (Suresh and Nangia, 2018; Sanphui and Bolla, 2018; He et al., 2019). CUR and n-acetylcysteine coformer using the supercritical solvent method indicated the cocrystal formation with higher solubility than the initial CUR (Paulazzi et al., 2022). CUR can also form cocrystals with ascorbic acid coformer by solvent evaporation, where the solubility can also increase significantly compared to the initial CUR (Pantwalawalkar et al., 2021). CUR cocrystallization was carried out with isonicotinamide (INIC) as a coformer by solvent evaporation. INIC was chosen as a coformer because structurally, it has amide groups and furan rings, so it has the potential to form short-strong hydrogen bonds with hydroxyl groups on CUR molecules (Kerr et al., 2015). In addition, INIC is easily soluble in water, so it is likely to increase the solubility of the resulting cocrystal (Suresh and Nangia, 2018).

2. EXPERIMENTAL SECTION

2.1 Chemicals and Equipment

The chemicals used were CUR (Tokyo Chemical Industry Co., Ltd.), INIC (Sigma-Aldrich®), CMC-Na (Merck®), carrageenan (Sigma-Aldrich®), and methanol (PT. Smart Lab Indonesia). The experimental animals used were male BALB/c rats (20-30 g) obtained from the Faculty of Dentistry University of Jember. The research equipment used was a powder X-ray diffractometer (PXRD), a differential scanning calorimeter (DSC), a Fourier-transform infrared spectrometer (FTIR), a scanning electron microscope (SEM) equipped with an ion sputter, a UV-Vis spectrophotometer, a magnetic stirrer, and an orbit shaker.

2.2 Methods

2.2.1 Cocrystallization of CUR-INIC

CUR and INIC in an equimolar ratio (1:1) were put into a beaker (total weight 1 g). 10 mL of methanol was added to the beaker glass, then tightly closed with aluminum foil. The mixture in the beaker glass was then stirred with a magnetic stirrer (Thermo Fisher SP88857107) at 300 rpm (30°C) for 30 minutes, and after that, the aluminum foil covering the beaker glass was given small holes. The beaker was gently shaken with an orbital shaker (Thermo Scientific) at 125 rpm (30°C) so that the solvent evaporated, leaving the solid. The dry solids were then reduced with a mortar and sieved through an 80-mesh sieve.

2.2.2 Characterization with PXRD

Tests were carried out with a PANalytical X'Pert Pro diffractometer using CuKα1 (λ=1.542 Å) as a radiation source. Scanning at an angle of 2β with a speed of 10°/min uses a size range of 5-50° with a voltage of 40 kV and a current of 30 mA.

2.2.3 Characterization with DSC

The equipment used was Thermo plus EVO DSC 8230. The sample (approximately 2 mg) was put into an airtight aluminum pan and closed tightly with a press apparatus. The sample is then placed on the sample board on the DSC. The DSC test was carried out under dry airflow conditions with a temperature range of 30-200°C and a heating rate of 10°C/minute.

2.2.4 Characterization with FTIR

FTIR spectra were determined using a Fourier transform infrared spectrometer (Thermo Scientific Nicolet iS10). A sample of about 5 mg was sprinkled evenly on the board from the equipment, and then measurements were taken using a resolution of 4 cm^{-1} at a wave number of 4000-600 cm^{-1}.

2.2.5 Characterization with SEM

The equipment used is a Hitachi TM 3000 with an ion sputter (Hitachi E-1045). The sample powder was placed evenly on the sample board, then coated with platinum using an ion sputter for 20 seconds. Then the samples were observed using SEM at a voltage of 15 kV and a current of 30 mA with the appropriate magnification.

2.2.6 Solubility Test

The solubility test using an excess sample (about 20 mg) was carried out by shaking method. Samples were containerized with Erlenmeyer, and added 10 mL of distilled water. Then the Erlenmeyer was tightly closed using aluminum foil and shaken for 24 hours using an orbital shaker (Thermo Scientific) at 175 rpm (30°C). The supernatant was filtered (0.45 microns) and diluted with sufficient methanol, and then the CUR level was measured using a UV-Vis spectrophotometer at λ 425 nm (Thermo Scientific Genesys 20). The solubility test was repeated thrice (Hanif et al., 2022).

2.2.7 Evaluation of Anti-Inflammatory Activity

Anti-inflammatory activity was evaluated using the mice-carrageenan-induced paw edema method (Gupta et al., 2015; Ahangar et al., 2019; Yimer et al., 2020). The experimental animal treatment procedure was approved by the Research Ethics Committee of the University of Jember (No. 1360/UN25.8/KEPK/DL/2021). Male BALB/c mice (20-30 g) were grouped into three (6 mice each): the control group (I), the pure CUR group (II), and the CUR-INIC group (III) (Ma et al., 2019; Zhnyakina et al., 2020). Mice were acclimatized for seven days by being given water and a standard diet ad libitum under standard conditions. Before being treated, the mice fasted for 12 hours (no diet but still given water).

Treatment was given by gavage, 0.5% CMC-Na suspension (0.1 mL/kg BW) to group I (control group), 0.5% CMC Na suspension containing CUR (dose 200 mg/kg BW) to group II, and 0.5% CMC Na suspension containing CUR-INIC (dose equivalent to CUR of 200 mg/kg BW) to group III. After administration of the suspension, the thickness of the right hind paw of the mice was measured with a caliper (T0). One hour after administration of the suspension, the right hind paw of the mice (sub-plantar area) was injected with 0.01 mL of 1% carrageenan. Furthermore, after 0.5, 1, 2, 3, 4, and 5 hours of 1% carrageenan treatment, the thickness of the right hind paw of the mice has measured again (Tt). The changes in the thickness of the paw (Δ) were calculated as the difference between the paw thickness after injection (Tt) and the paw thickness before injection (T0). The percentage of edema inhibition (5 hours after injection of 1% carrageenan) was calculated by the formula: % edema inhibition = [(Δcontrol-Δtreatment)/Δcontrol] × 100 (Gupta et al., 2015).

2.2.8 Statistical Analysis

Statistical analysis was carried out using one-way ANOVA and Bonferroni post hoc test on the SPSS 22.0 software program. Differences in data between sample groups were considered significant if the p-value<0.05.

3. RESULTS AND DISCUSSION

3.1 PXRD Diffractogram

The PXRD diffractograms of CUR, INIC, and CUR-INIC are shown in Figure 1. The PXRD diffractograms of CUR have shown sharp peaks at 7.75, 8.72, 15.72, 17.06, and 20.98°, indicating similarity to the diffractogram of the CUR polymorph form 1, which has a monoclinic crystal structure (Sanphui et al., 2011). INIC has shown a diffractogram with sharp peaks at 7.59, 20.60, 25.66, 26.38, and 30.74°, which indicates agreement with the literature (Liu et al., 2021).

The solid CUR-INIC has a PXRD diffractogram with a new pattern different from the CUR and INIC diffractograms. New diffraction peaks appear on the CUR-INC diffractogram, namely at 15.00, 16.22, and 22.89°. The presence of new peaks on the CUR-INIC diffractogram indicates that the solid CUR-INIC is not a physical mixture of CUR and INIC but is a new crystalline solid with a different structure resulting from the interaction between CUR and INIC (Pantwalawalkar et al., 2021).

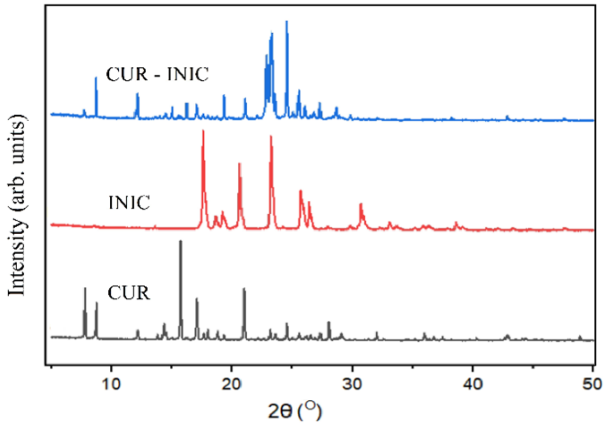

Figure 1. PXRD Difractogram of (a) CUR, (b) INIC, and (c) CUR-INIC

3.2 DSC Thermogram

The DSC thermograms of CUR, INIC, and CUR-INIC are shown in Figure 2. The thermogram of CUR shows an endothermic peak at 186.1°C (ΔH = 119.25 J/g), while the thermogram of INIC also shows an endothermic peak at 156.9°C (ΔH = 175.24 J/g). The temperatures of the endothermic peaks on the CUR and INIC thermograms are correlated with melting points that agree with the literature Ketkar et al. (2016) and Abdelkader et al. (2022).

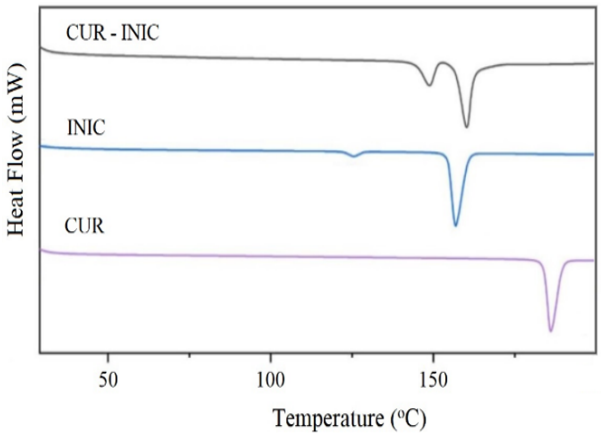

Figure 2. DSC Thermogram of (a) CUR, (b) INIC, and (c) CUR-INIC

On the CUR-INIC thermogram, two endothermic peaks appear, namely at 149.2°C (ΔH = 32.742 J/g) and 160.1°C (ΔH = 76.344 J/g). The first endothermic peak (149.2°C) represents the melting of the eutectic mixture, while the second endothermic peak (160.1°C) represents the melting of the CUR-INIC cocrystal (Pantwalawalkar et al., 2021). The CUR-

INIC cocrystal solid showed melting at temperatures between the melting temperatures of CUR and INIC, indicating that CUR and INIC molecules formed intermolecular interactions in CUR-INIC solids with a different arrangement compared to CUR and INIC, resulting in a new crystalline solid phase (Satapathy et al., 2021).

The molecular arrangement of CUR-INIC cocrystal solids determines the formation of crystal packing and crystal lattice energy in CUR-INIC cocrystal solids (Kilinkissa et al., 2020; Volodin et al., 2019; Ejarque et al., 2021). Packing and crystal lattice energy affect the melting temperature of the solids, and cocrystals generally have melting temperatures between those of their constituents (Qiao et al., 2011; Salahinejad et al., 2013; Gamidi et al., 2018). The CUR- INIC cocrystal exhibits a lower melting point than pure CUR solids because the INIC molecules in the cocrystal structure are thought to produce a repeating pattern of the crystal lattice with more significant variations in intermolecular forces, thereby lowering the melting point (Salahinejad et al., 2013; Gamidi et al., 2018). The pattern of the thermogram and melting point of the CUR-INIC cocrystal shows similarities to the CUR-ascorbic acid cocrystal (Pantwalawalkar et al., 2021).

3.3 FTIR Spectra

The FTIR spectra of CUR, INIC, and CUR-INIC are shown in Figure 3. The CUR spectra showed an absorption peak at 3500 cm^{-1}, indicating stretching vibrations of O-H phenolic, 1626 cm^{-1} associated with stretching vibrations of C=C and C=O, 1601 cm^{-1} associated with C=C stretching vibrations of the aromatic ring, 1505 cm^{-1} associated with vibrations of C=O, 1262 cm^{-1} associated with vibrations of aromatic C-O (enol groups), and 1026 cm^{-1} associated with vibrations of C-O-C group (Sharma et al., 2022). INIC has a spectrum with absorption peaks at 3363 and 3177 cm^{-1}, showing stretching vibrations of asymmetric and asymmetric N-H, 1657 cm^{-1} associated with stretching vibrations of C=O amide, 1621 cm^{-1} associated with bending vibrations of amide N-H, and 1408 cm^{-1} is related to the stretching vibrations of C-N amide (Ferreira et al., 2022).

In the CUR-INIC spectra, it appears as a combination of the absorption peaks from the CUR and INIC spectra. However, there were shifts in wave number values at several absorption peaks compared to the individual absorption peaks of CUR and INIC. The CUR absorption peaks in the CUR-INIC spectra, which showed a shift, were 3500 to 3507 cm^{-1}, 1262 to 1275 cm^{-1}, and 1026 to 985 cm^{-1}. Meanwhile, the absorption peaks of INIC in the CUR-INIC spectra showed a shift, 3363 to 3329 cm^{-1}, 1657 to 1679 cm^{-1}, 1621 to 1626 cm^{-1}, and 1408 to 1413 cm^{-1}. The absorption peaks of CUR-INIC, which are experiencing a shift, are the absorption peaks of the donor and acceptor groups of hydrogen bonds. The shift of the absorption peaks indicates that in CUR- INIC, there has been a hydrogen bonding interaction involving the phenolic O-H, aromatic C-O (enol), and C-O-C groups of the CUR molecules with the C=O, N-H, and C-N groups of the INIC molecules (Pantwalawalkar et al., 2021).

3.4 SEM Images

SEM is useful for analyzing the morphology and surface topography of materials. SEM images of CUR, INIC, and CUR-INIC are shown in Figure 4. SEM images have shown that the shape of the CUR particles is a rectangular plate with a smooth surface, while the shape of the INIC particles is a rod with a wavy surface. SEM images of CUR-INIC particles have shown a different shape and appearance than CUR and INIC particles. CUR-INIC particles have an irregular shape resulting from aggregating a set of particles, and there are no visible traces of CUR and INIC particles. The aggregates of CUR-INIC particles form a morphology and surface topography with a hollow structure indicating a larger surface area. The characteristics of particles with a hollow structure generally have more excellent solubility properties than particles with a dense structure (Agarwal et al., 2020; Kawano et al., 2021).

Based on the results of the analysis with PXRD, DSC, FTIR, and SEM, it was concluded that CUR and INIC, after preparation, formed a new solid phase with a different molecular arrangement compared to the starting material. The CUR and INIC molecules in the CUR-INIC solid form a hydrogen bond interaction, resulting in a new crystal structure. The new crystal structure of the CUR-INIC cocrystal is indicated in the PXRD diffractogram and FTIR spectra. The CUR-INIC cocrystal shows different thermodynamic and physical properties compared to each constituent material, as shown in the analysis results by DSC and SEM.

3.5 Solubility

The nature of solubility in water is a critical parameter that determines the absorption and bioavailability of an API. CUR is poorly soluble in water, so it is difficult to absorb by the gastrointestinal tract, causing its bioavailability to be below 1% (Suresh and Nangia, 2018; Peng et al., 2021). The solubility test results showed that CUR had a solubility in water of 5.05±0.07 μg/mL, while the CUR-INIC cocrystal in the water had a solubility of 73.1±0.23 μg/mL. These results indicated that the cocrystallization of CUR-INIC has increased the solubility of CUR about 14 times.

The solubility of a crystalline solid is strongly influenced by its crystal structure and packing, which is related to the crystal lattice energy. Crystalline solids with lower lattice energy are made up of molecules bonded with weaker energy, and during the dissolution process, water molecules more easily hydrate them (Kuleshova et al., 2013; Thakuria et al., 2013). Cocrystals are formed from molecules of API and coformer that make up the crystal lattice. Molecules of API and coformer in cocrystals interact with non-covalent bonds, such as hydrogen bonds, forming new structures and packings with different lattice energies than the starting materials (Guo et al., 2018).

Based on the results of the diffractogram, the CUR used in this study is a CUR polymorph form 1 with a monoclinic structure known to have very low water solubility (Sanphui

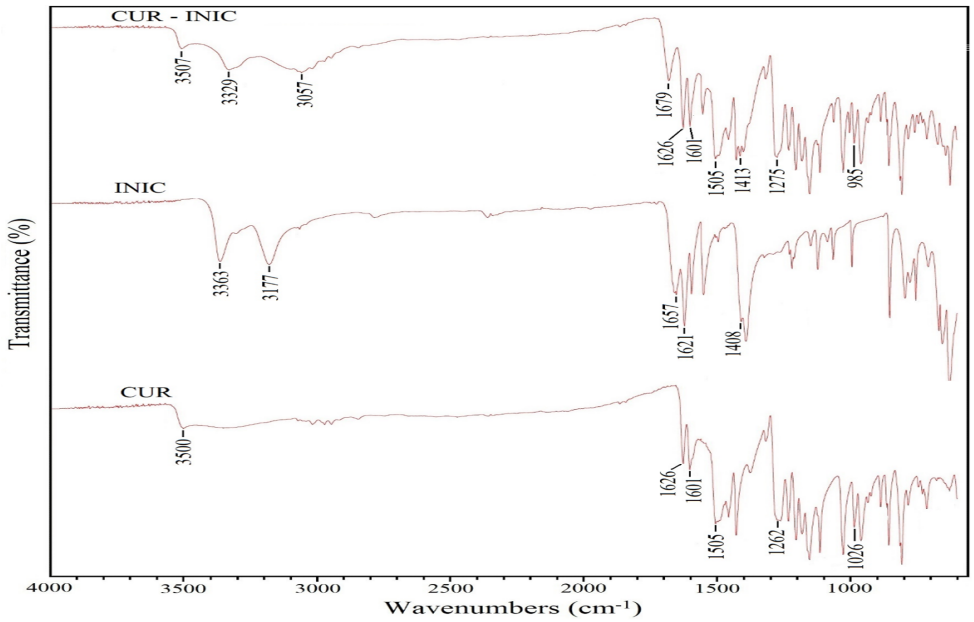

Figure 3. FTIR Spectra of (a) CUR, (b) INIC, and (c) CUR-INIC

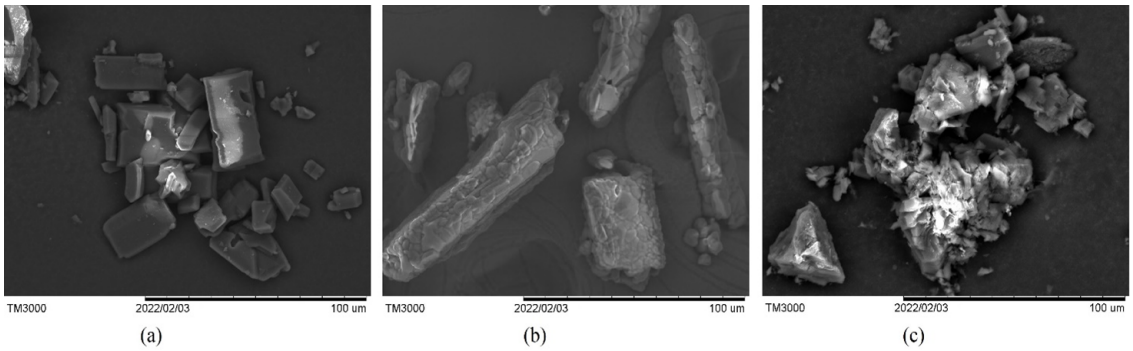

Figure 4. SEM Images of (a) CUR, (b) INIC, and (c) CUR-INIC (15 kV, ×1000)

et al., 2011). Sanphui et al. (2011) modified the CUR crystal form and produced CUR polymorph forms 2 and 3 with an orthorhombic structure with a higher dissolution rate than CUR form 1 (monoclinic). CUR in the CUR-INIC cocrystal exhibited a higher solubility than the initial CUR, presumably due to lowering the crystal lattice energy of the CUR-INIC cocrystal. The intermolecular interaction of INIC with CUR changes the structure and arrangement of the crystal lattice of CUR so that the cocrystal solid formed has a lower lattice energy. Cocrystals with lower lattice energy become more easily hydrated by water molecules, increasing their solubility and dissolution rate (Ozaki et al., 2014; Docherty et al., 2015; Bergström and Larsson, 2018).

3.6 Anti-Inflammatory Activity

Changes in the paw thickness of mice after being induced with 1% carrageenan are shown in Figure 5. Changes in paw thickness indicate the occurrence of edema, which correlates with inflammation. In group I (control), changes in paw thickness occurred after 1% carrageenan administration, increased until the 4th hour, and then decreased at the 5^{th} hour. In groups II (CUR group) and III (CUR-INIC group), the paw thickness increased until about 1 hour after 1% carrageenan administration. Then the paw thickness decreased until the 5th hour. Changes in paw thickness of group I (control) at 1 to 5 hours showed a significant difference ($p<0.05$) compared to changes in paw thickness from the II and III groups. The changes in paw thickness show that administration of 1% carrageenan has induced edema in all groups of mice. In II and III groups, there was a significant ($p<0.05$) decrease in edema (at 1 to 5 hours) compared to group I (control) as a result of the administration of CUR and CUR-INIC cocrystals. The decrease in edema has proven that administering CUR and CUR-INIC cocrystals in II and III groups has an anti-inflammatory effect in mice.

The percentage of edema inhibition at 5 hours showed that in the II group (CUR), there was an inhibition of edema of

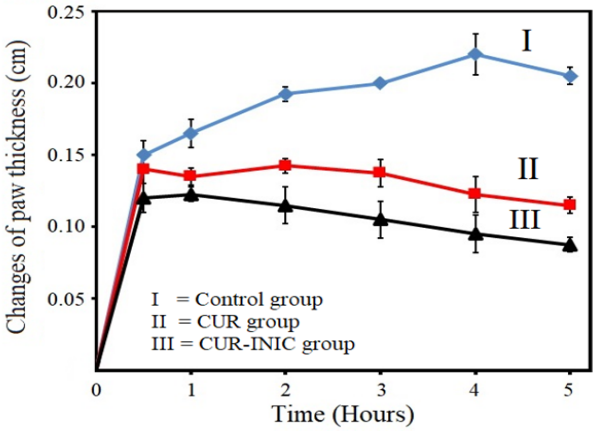

Figure 5. Changes of the Paw Thickness of Mice of (a) Control Group, (b) CUR Group, and (c) CUR-INIC Group

43.90±2.82%, while in the III group (CUR-INIC cocrystal), there was an inhibition of edema of 57.32±2.44%. The percentage of edema inhibition indicates that administration of CUR in the form of CUR-INIC cocrystals (equivalent to CUR 200 mg/kg BW) had significantly higher inhibition (130%) of edema than administration of initial CUR without cocrystallization.

The solubility of the CUR-INIC cocrystal increased significantly ($p<0.05$) compared to the solubility of the initial CUR. The increase in the solubility of the CUR-INIC cocrystal is thought to cause the amount of dissolved CUR in the digestive tract of mice to be greater than that of group II (CUR). The amount of API dissolved in the digestive tract is generally directly proportional to the API absorbed, which has a pharmacological effect (Khames, 2017). Thus, it can be estimated that the increased anti-inflammatory activity in group III (CUR-INIC cocrystal) compared to group II (CUR) is due to the increased solubility of CUR in the CUR-INIC cocrystal (Granata et al., 2017; He et al., 2019).

4. CONCLUSIONS

Cocrystallization of CUR with INIC coformer produces CUR-INIC cocrystals, which exhibit novel crystalline solid characteristics. The PXRD diffractogram of the CUR-INIC cocrystal has a different pattern of diffraction peaks compared to the individual diffractograms of CUR and INIC. The molecules of the constituent materials in the CUR-INIC cocrystal form intermolecular interactions of hydrogen bonds which produce a new solid phase with a melting point of 160.1°C. The CUR-INIC cocrystal showed a solubility in water of 73.1±0.23 μg/mL. In comparison, the initial CUR showed a solubility of only 5.05±0.07 μg/mL, so the cocrystallization of CUR with INIC coformer could increase the solubility of CUR by 14 times. CUR-INIC cocrystal showed anti-inflammatory activity in mice 130% stronger than initial CUR. Thus, increasing the solubility of CUR through forming CUR-INIC cocrystals is an opportunity for further development to obtain CUR with a more potent anti-inflammatory effect.

5. ACKNOWLEDGMENT

The researchers express gratitude to the Rector of the University of Jember for the funds provided through the IDB Supporting Research Grant based on the Rector Decree Number: 14970/UN25/KP/2022 and Assignment Agreement Number: 4400/UN25.3.1/LT/2022.

REFERENCES

Abdelkader, H., A. A. Fatease, Z. Fathalla, M. E. Shoman, H. A. Abou-Taleb, and M. A. Abourehab (2022). Design, Preparation and Evaluation of Supramolecular Complexes with Curcumin for Enhanced Cytotoxicity in Breast Cancer Cell Lines. *Pharmaceutics*, **14**(11); 2283

Acebedo-Martínez, F. J., C. Alarcón-Payer, H. M. Barrales-Ruiz, J. Niclós-Gutiérrez, A. Domínguez-Martín, and D. Choquesillo-Lazarte (2022). Towards the Development of Novel Diclofenac Multicomponent Pharmaceutical Solids. *Crystals*, **12**(8); 1038

Agarwal, A., A. Mittal, S. Ikram, L. Tyagi, and C. Gupta (2020). Solubility Enhancement of Nicergoline Poorly Water Soluble Drug by Novel Melt Sonocrystallization Technique. *Scholars Academic Journal of Pharmacy*, **9**(12); 347–365

Ahangar, N., F. Mirzaee, M. Feizbakhsh, S. Pirhayati, and S. Shahani (2019). Antinociceptive and Anti-Inflammatory Effects of *Geum iranicum khatamsaz* Methanol Extract in Mice. *Research Journal of Pharmacognosy*, **6**(3); 41–9

Anggraini, D., H. Salsabila, S. Umar, Y. Aldi, and E. Zaini (2022). Preparation and Characterization of a Eutectic Mixture of Fenofibric Acid and Nicotinic Acid and Evaluatuion of In Vivo Antihyperlipidemic Activity. *Science and Technology Indonesia*, **7**(4); 514–521

Bergström, C. A. and P. Larsson (2018). Computational Prediction of Drug Solubility in Water-Based Systems: Qualitative and Quantitative Approaches used in the Current Drug Discovery and Development Setting. *International Journal of Pharmaceutics*, **540**(1-2); 185–193

Chavan, R. B. and N. R. Shastri (2018). Overview of Multicomponent Solid Forms. *Journal of Nanotoxicology and Nanomedicine*, **3**(1); 23–48

Chen, Y., Y. Lu, R. J. Lee, and G. Xiang (2020). Nano Encapsulated Curcumin: and its Potential for Biomedical Applications. *International Journal of Nanomedicine*, **15**; 3099–3120

Docherty, R., K. Pencheva, and Y. A. Abramov (2015). Low Solubility in Drug Development: De-Convoluting the Relative Importance of Solvation and Crystal Packing. *Journal of Pharmacy and Pharmacology*, **67**(6); 847–856

Ejarque, D., T. Calvet, M. Font-Bardia, and J. Pons (2021). Cocrystals Based on 4, 4'-Bipyridine: Influence of Crystal Packing on Melting Point. *Crystals*, **11**(2); 191

Fang, L., Y. Xiao, C. Zhang, Z. Gao, S. Wu, J. Gong, and S. Rohani (2021). Intermolecular Interactions and Solubil-

ity Behavior of Multicomponent Crystal Forms of 2, 4-D: Design, Structure Analysis, and Solid-State Characterization. *CrystEngComm*, **23**(43); 7615–7627

Ferreira, P. O., F. J. Caires, F. Z. R. de Souza, R. P. Fernandes, and A. C. de Almeida (2022). Screening of Coformers for Quercetin Cocrystals Through Mechanochemical Methods. *Eclética Química*, **47**(1); 64–75

Fischer, F., A. Heidrich, S. Greiser, S. Benemann, K. Rademann, and F. Emmerling (2016). Polymorphism of Mechanochemically Synthesized Cocrystals: A Case Study. *Crystal Growth & Design*, **16**(3); 1701–1707

Gamidi, R. K., M. Ukrainczyk, J. Zeglinski, and Å. C. Rasmuson (2018). Prediction of Solid State Properties of Co-Crystals using Artificial Neural Network Modelling. *Crystal Growth & Design*, **18**; 133–144

Gao, Y., G. Chen, X. Luan, M. Zou, H. Piao, and G. Cheng (2019). Improved Oral Absorption of Poorly Soluble Curcumin Via the Concomitant use of Borneol. *AAPS PharmSciTech*, **20**; 1–10

Granata, G., I. Paterniti, C. Geraci, F. Cunsolo, E. Esposito, M. Cordaro, A. R. Blanco, S. Cuzzocrea, and G. M. Consoli (2017). Potential Eye Drop Based on a Calix [4] Arene Nanoassembly for Curcumin Delivery: Enhanced Drug Solubility, Stability, and Anti-Inflammatory Effect. *Molecular Pharmaceutics*, **14**(5); 1610–1622

Guo, M., X. Sun, J. Chen, and T. Cai (2021). Pharmaceutical Cocrystals: A Review of Preparations, Physicochemical Properties and Applications. *Acta Pharmaceutica Sinica B*, **11**(8); 2537–2564

Guo, W., S. Du, Y. Lin, B. Lu, C. Yang, J. Wang, and Y. Zeng (2018). Structural and Computational Insights Into the Enhanced Solubility of Dipfluzine by Complexation: Salt and Salt-Cocrystal. *New Journal of Chemistry*, **42**(18); 15068–15078

Gupta, A. K., D. Parasar, A. Sagar, V. Choudhary, B. S. Chopra, R. Garg, Ashish, and N. Khatri (2015). Analgesic and Anti-Inflammatory Properties of Gelsolin in Acetic Acid Induced Writhing, Tail Immersion and Carrageenan Induced Paw Adema in Mice. *PloS one*, **10**(8); e0135558

Hakim, L., D. Mardiana, U. Rokhiyah, M. L. A. D. Lestari, and Z. Ningsih (2021). Structure and Dynamics of Curcumin Encapsulated Lecithin Micelles: A Molecular Dynamics Simulation Study. *Science and Technology Indonesia*, **6**(3); 113–120

Haneef, J., S. Ali, and R. Chadha (2021). Emerging Multi-Drug Eutectics: Opportunities and Challenges. *AAPS PharmSciTech*, **22**; 1–17

Haneef, J. and R. Chadha (2017). Drug-Drug Multicomponent Solid Forms: Cocrystal, Coamorphous and Eutectic of Three Poorly Soluble Antihypertensive Drugs using Mechanochemical Approach. *AAPS PharmSciTech*, **18**; 2279–2290

Hanif, M., N. Ameer, Q.-u.-A. Ahmad, M. Aziz, K. Mahmood, N. Ramzan, and H. M. Abdur Rahman (2022). Improved Solubility and Corneal Permeation of PEGylated Curcumin Complex used for the Treatment of Ophthalmic Bacterial Infections. *Plos one*, **17**(4); e0258355

He, Y., H. Liu, W. Bian, Y. Liu, X. Liu, S. Ma, X. Zheng, Z. Du, K. Zhang, and D. Ouyang (2019). Molecular Interactions for the Curcumin-Polymer Complex with Enhanced Anti-Inflammatory Effects. *Pharmaceutics*, **11**(9); 442

Karimi-Jafari, M., L. Padrela, G. M. Walker, and D. M. Croker (2018). Creating Cocrystals: A Review of Pharmaceutical Cocrystal Preparation Routes and Applications. *Crystal Growth & Design*, **18**(10); 6370–6387

Kawano, Y., S. Chen, and T. Hanawa (2021). Solubility Enhancement of Ibuprofen by Adsorption onto Spherical Porous Calcium Silicate. *Pharmaceutics*, **13**(6); 767

Kerr, H. E., L. K. Softley, K. Suresh, A. Nangia, P. Hodgkinson, and I. R. Evans (2015). A Furosemide–Isonicotinamide Cocrystal: An Investigation of Properties and Extensive Structural Disorder. *CrystEngComm*, **17**(35); 6707–6715

Ketkar, S., S. K. Pagire, N. R. Goud, K. Mahadik, A. Nangia, and A. Paradkar (2016). Tracing the Architecture of Caffeic Acid Phenethyl Ester Cocrystals: Studies on Crystal Structure, Solubility, and Bioavailability Implications. *Crystal Growth & Design*, **16**(10); 5710–5716

Khames, A. (2017). Investigation of the Effect of Solubility Increase at the Main Absorption Site on Bioavailability of BCS Class II Drug (Risperidone) using Liquisolid Technique. *Drug Delivery*, **24**(1); 328–338

Kilinkissa, O. E., K. K. Govender, and N. B. Báthori (2020). Melting Point–Solubility–Structure Correlations in Chiral and Racemic Model Cocrystals. *CrystEngComm*, **22**(16); 2766–2771

Kuleshova, L., D. Hofmann, and R. Boese (2013). Lattice Energy Calculation–a Quick Tool for Screening of Cocrystals and Estimation of Relative Solubility. Case of Flavonoids. *Chemical Physics Letters*, **564**; 26–32

Liu, H., H. Lin, Z. Zhou, and L. Li (2021). Bergenin-Isonicotinamide (1:1) Cocrystal with Enhanced Solubility and Investigation of its Solubility Behavior. *Journal of Drug Delivery Science and Technology*, **64**; 102556

Ma, X. Q., C. Zhuang, B. C. Wang, Y. F. Huang, Q. Chen, and N. Lin (2019). Cocrystal of Apigenin with Higher Solubility, Enhanced Oral Bioavailability, and Anti-Inflammatory Effect. *Crystal Growth & Design*, **19**(10); 5531–5537

Maheshwari, C., A. Jayasankar, N. A. Khan, G. E. Amidon, and N. Rodríguez-Hornedo (2009). Factors that Influence the Spontaneous Formation of Pharmaceutical Cocrystals by Simply Mixing Solid Reactants. *CrystEngComm*, **11**(3); 493–500

Ozaki, S., Y. Nakagawa, O. Shirai, and K. Kano (2014). Substituent Effect on the Thermodynamic Solubility of Structural Analogs: Relative Contribution of Crystal Packing and Hydration. *Journal of Pharmaceutical Sciences*, **103**(11); 3524–3531

Palanisamy, V., P. Sanphui, M. Prakash, and V. Chernyshev (2019). Multicomponent Solid Forms of the Uric Acid Reabsorption Inhibitor Lesinurad and Cocrystal Polymorphs with

Urea: DFT Simulation and Solubility Study. *Acta Crystallographica Section C: Structural Chemistry*, **75**(8); 1102–1117

Pantwalawalkar, J., H. More, D. Bhange, U. Patil, and N. Jadhav (2021). Novel Curcumin Ascorbic Acid Cocrystal for Improved Solubility. *Journal of Drug Delivery Science and Technology*, **61**; 102233

Paulazzi, A. R., B. O. Alves, G. A. Zilli, A. E. Dos Santos, F. Petry, K. D. Soares, L. J. Danielli, J. Pedroso, M. A. Apel, and G. P. S. Aguiar (2022). Curcumin and n-Acetylcysteine Cocrystal Produced with Supercritical Solvent: Characterization, Solubility, and Preclinical Evaluation of Antinociceptive and Anti-Inflammatory Activities. *Inflammopharmacology*, **30**(1); 327–341

Peng, Y., M. Ao, B. Dong, Y. Jiang, L. Yu, Z. Chen, C. Hu, and R. Xu (2021). Anti-Inflammatory Effects of Curcumin in the Inflammatory Diseases: Status, Limitations and Countermeasures. *Drug Design, Development and Therapy*; 4503–4525

Priyadarsini, K. I. (2014). The Chemistry of Curcumin: From Extraction to Therapeutic Agent. *Molecules*, **19**(12); 20091–20112

Qiao, N., M. Li, W. Schlindwein, N. Malek, A. Davies, and G. Trappitt (2011). Pharmaceutical Cocrystals: An Overview. *International Journal of Pharmaceutics*, **419**(1-2); 1–11

Salahinejad, M., T. C. Le, and D. A. Winkler (2013). Capturing the Crystal: Prediction of Enthalpy of Sublimation, Crystal Lattice Energy, and Melting Points of Organic Compounds. *Journal of Chemical Information and Modeling*, **53**(1); 223–229

Sanphui, P. and G. Bolla (2018). Curcumin, a Biological Wonder Molecule: A Crystal Engineering Point of View. *Crystal Growth & Design*, **18**(9); 5690–5711

Sanphui, P., N. R. Goud, U. R. Khandavilli, S. Bhanoth, and A. Nangia (2011). New Polymorphs of Curcumin. *Chemical Communications*, **47**(17); 5013–5015

Satapathy, B. S., A. Patel, R. N. Sahoo, and S. Mallick (2021). Crystal Products of Lamotrigine-Citric Acid for Improvement of in Vitro Drug Release in Simulated Gastric Fluid. *Journal of the Serbian Chemical Society*, **86**(1); 51–61

Sharma, M., B. S. Inbaraj, P. K. Dikkala, K. Sridhar, A. N. Mude, and K. Narsaiah (2022). Preparation of Curcumin Hydrogel Beads for the Development of Functional Kulfi: A Tailoring Delivery System. *Foods*, **11**(2); 182

Sohn, S.-I., A. Priya, B. Balasubramaniam, P. Muthuramalingam, C. Sivasankar, A. Selvaraj, A. Valliammai, R. Jothi, and S. Pandian (2021). Biomedical Applications and Bioavailability of Curcumin—An Updated Overview. *Pharmaceutics*, **13**(12); 2102

Suresh, K. and A. Nangia (2018). Curcumin: Pharmaceutical Solids as a Platform to Improve Solubility and Bioavailability. *CrystEngComm*, **20**(24); 3277–3296

Tabanelli, R., S. Brogi, and V. Calderone (2021). Improving Curcumin Bioavailability: Current Strategies and Future Perspectives. *Pharmaceutics*, **13**(10); 1715

Taylor, C. R. and G. M. Day (2018). Evaluating the Energetic Driving Force for Cocrystal Formation. *Crystal Growth & Design*, **18**(2); 892–904

Thakuria, R., A. Delori, W. Jones, M. P. Lipert, L. Roy, and N. Rodríguez-Hornedo (2013). Pharmaceutical Cocrystals and Poorly Soluble Drugs. *International Journal of Pharmaceutics*, **453**(1); 101–125

Volodin, A. D., A. A. Korlyukov, and A. F. Smol'yakov (2019). Organoelement Compounds Crystallized In Situ: Weak Intermolecular Interactions and Lattice Energies. *Crystals*, **10**(1); 15

Wicaksono, Y., V. A. Rosidi, S. Y. Saragih, L. S. Fauziah, and D. Setyawan (2021). Preparation of Spray Dried Coamorphous Solids to Improve the Solubility and Dissolution Rate of Atorvastatin Calcium. *Jurnal Teknologi*, **83**(2); 77–83

Wicaksono, Y., D. Setyawan, and A. S. Nugraha (2020). Kelakuan Termal Kokristal: Kajian Kes Kokristal Ketoprofen-Asid Malonik dan Ketoprofen-Nikotinamida. *Sains Malaysiana*, **49**(11); 2679–2687 (in Malaysia)

Yimer, T., E. M. Birru, M. Adugna, M. Geta, and Y. K. Emiru (2020). Evaluation of Analgesic and Anti-Inflammatory Activities of 80% Methanol Root Extract of *Echinops kebericho* M. (Asteraceae). *Journal of Inflammation Research*, **13**; 647–658

Zhang, J., Y. Zhang, H. Wang, W. Chen, A. Lu, H. Li, L. Kang, and C. Wu (2023). Solubilisation and Enhanced Oral Absorption of Curcumin using a Natural Non-Nutritive Sweetener Mogroside V. *International Journal of Nanomedicine*, **18**; 1031–1045

Zhnyakina, L., M. Tkachenko, Y. V. Moshchenskii, and I. Munina (2020). Differential Scanning Calorimetry Study of the Ibuprofen–Nicotinamide Binary Disperse System and the Anti-Inflammatory Activity of One of Its Secondary Eutectics. *Pharmaceutical Chemistry Journal*, **54**; 954–958

